C. R. Chimie 20 (2017) 78–86

Contents lists available at ScienceDirect

Comptes Rendus Chimie

www.sciencedirect.com

Full paper/Mémoire

Transformation of South African coal fly ash into ZSM-5 zeolite and its application as an MTO catalyst

Roland Na M. Missengue [a, *], Pit Losch [b], Grant Sedres [a], Nicholas M. Musyoka [c], Ojo O. Fatoba [a], Benoit Louis [b, **], Patrick Pale [b], Leslie F. Petrik [a]

[a] Department of Chemistry, University of the Western Cape, Cape Town, South Africa
[b] Department of Chemistry, University of Strasbourg, Strasbourg, France
[c] Council for Scientific and Industrial Research, Pretoria, South Africa

ARTICLE INFO

Article history:
Received 1 November 2015
Accepted 28 April 2016
Available online 11 October 2016

Keywords:
Fly ash
Acid leaching
Metal extraction
ZSM-5 zeolite
MTO catalyst

ABSTRACT

This study presents a way of using South African coal fly ash by extracting metals such as Al and Fe with concentrated sulphuric acid, and then using the solid residue as a feedstock for the synthesis of ZSM-5 zeolite. The percentage of aluminium and iron oxides decreased from $28.0 \pm 0.2\%$ and $5.0 \pm 0.1\%$ in coal fly ash to $24.6 \pm 0.1\%$ and $1.6 \pm 0.01\%$ in the acid treated coal fly ash respectively. The fly ash-based zeolite ZSM-5 sample synthesised from the solid residue after extraction of Al and Fe, contained 62% of ZSM-5 zeolite pure phase with a number of Brønsted acid site density of 0.61 mmol per $g_{zeolite}$.
By properly treating the as-prepared coal fly ash-based ZSM-5 zeolite, an active and selective methanol-to-olefins acid catalyst could be designed, leading to full methanol conversion during 15 h on stream. The optimised catalyst exhibited a cumulative methanol conversion capacity of 71 g($MeOH_{converted}$)/g(catalyst) and a light olefin productivity of 21 g($C_{2=}$–$C_{4=}$)/g(catalyst).

Mots-clés:
Cendres volantes
Lixiviation acide
Extraction de métal
Zéolithe ZSM-5
Catalyseur de conversion du méthanol en oléfines légères

RÉSUMÉ

Cette étude présente une stratégie de valorisation de cendres du charbon (origine : Afrique du Sud) après extraction de métaux tels que le fer ou l'aluminium. Le résidu solide est ensuite utilisé comme matière première pour synthétiser une zéolithe ZSM-5. Cette dernière est obtenue sous la forme d'un matériau composite zéolithe (62%)/cendre, présentant une acidité de Brønsted de 0,61 mmol par $g_{zeolite}$.
Par une conception sur mesure ou *rational design*, un composite ZSM-5/cendre s'est avéré être un catalyseur actif et sélectif dans la réaction de conversion du méthanol en oléfines légères (MTO). Une capacité totale de conversion du méthanol de 71 $g/g_{catalyseur}$ accompagnée d'une productivité de 21 g ($C_{2=}$–$C_{4=}$)/$g_{catalyseur}$ a ainsi été obtenue.

1. Introduction

Coal fly ash (FA) is an industrial by-product which is generated during energy production through coal combustion. FA mainly consists of SiO_2, Al_2O_3 and Fe_2O_3, but

* Corresponding author.
** Corresponding author.
E-mail addresses: rmissengue@gmail.com (R.N.M. Missengue), blouis@unistra.fr (B. Louis).

http://dx.doi.org/10.1016/j.crci.2016.04.012
1631-0748/

also contains potentially toxic elements such as heavy metals from coal and polyaromatic hydrocarbons that condense from the flue gas. The large-scale disposal and storage of FA is a source of air, soil and water pollution [1]. In order to minimize its disposal as wastes, FA has been used to treat acid mine drainage [2,3], to synthesize zeolites [2,4,5], as construction materials [1], or to recover valuable metals [6,7]. Two processes for alumina recovery from FA were developed in the seventies in Poland [8]. Nowadays, many processes such as sintering, acid leaching and HiChlor for alumina recovery from FA have been developed [9]. Regarding coal FA, Liu et al. reported the recovery of 70–90 % of the total alumina content from coal fly ash using acid sintering-leaching process with concentrated sulphuric acid [7]. Iron oxides can also be recovered from FA through magnetic extraction upon acidic treatment with aqueous sulphuric acid or hydrochloric acid [10,11].

Fly ash has been used as a low cost source of SiO_2, Al_2O_3 in the synthesis of zeolites [12]. For such syntheses, the conventional alkaline hydrothermal process could be applied, but after fusion or pectization of the raw material [4,13]. Under such conditions, A, X, Na–P1 and cancrinite zeolites have been successfully prepared from South African coal FA by Musyoka et al. [4,12].

The extraction of alumina from FA obviously leads to an increase in the Si/Al ratio of the solid residue, which might be a good starting material for the synthesis of high silica containing zeolites such as ZSM-5 (Si/Al $\geq$ 11) [14]. ZSM-5 zeolite, having the MFI topology with high silica content, exhibits a three-dimensional medium-sized pore structure, high temperature stability and strong acidity. It is a well-established catalyst for several petrochemical processes such as cracking, alkylation, acylation, disproportionation, isomerisation, *etc.* ZSM-5 zeolite is conventionally synthesised using various types of organic structure-directing agents [14–17]. However, Narayanan et al. reported that ZSM-5 could be synthesised without templates [18]. Chareonpanich et al. prepared ZSM-5 zeolite using lignite FA and rice husk ash as feedstocks, with tetrapropylammonium bromide (TPABr) as a template [5]. Kalyankar et al. obtained ZSM-5 zeolite using FA obtained from a thermal power station in India [19].

The conversion of methanol into hydrocarbons (MTH) for producing high-octane gasoline was discovered in Mobil laboratories in the 70s. This process now represents a valuable technology, based on acid-catalysed reactions, which is commercialised: for instance, the Topsøe integrated gasoline synthesis (TIGAS) process, the Lurgi methanol to propene (MTP) process and the Norsk Hydro/UOP's methanol to olefins (MTO) process [20]. For the latter process, Chang et al. [21c] reported that an increase in the Si/Al ratio led to an enhancement of the MTO catalyst activity. Furthermore, other key parameters that affect an MTO catalyst need to be controlled: crystal size, crystallinity and, as aforementioned, the intrinsic acidity in terms of density as well as strength [21]. It is therefore a challenge to transform a very complex waste material into a heterogeneous catalyst with tailored properties. Lastly, an interesting perspective for the study is the potential applicability of FA ZSM-5 zeolite, for instance, in China where Coal-To-Methanol processes are industrialized [21e]. Indeed, it is desirable that FA generated by the latter processes could be valorised in the design of an MTO catalyst.

Our study aims to show the potential use of South African coal fly ash as a cheap source for the extraction of metals and the synthesis of ZSM-5 zeolite, which is tested as an acid catalyst in the MTO reaction.

2. Experimental

2.1. Materials

Sulphuric acid (H_2SO_4, 95–99%) was purchased from Merck. Tetrapropylammonium bromide (TPABr), methanol (99.8%), chloroform-d ($CDCl_3$, 99 atom % D), chloroform ($CHCl_3$, ≥99.9%), oxalic acid ($H_2C_2O_4$, ≥99%) and fumed silica were obtained from Sigma-Aldrich. Sodium hydroxide (NaOH, pearls, 97%) was purchased from Kimix Chemical and Laboratory Supplies. Ammonium nitrate (NH_4NO_3) was obtained from Sigma–Aldrich. A commercial ZSM-5 zeolite (H-ZSM-5_{5524}) was purchased from Zeolyst. Fly ash (FA) was obtained from the Arnot coal power plant located in the Mpumalanga province of South Africa.

2.2. Acid leaching of fly ash and iron extraction

The acid leaching method used in this study was adapted from the method proposed by Liu et al. [7]. Fly ash (30 g) was mixed with 60 mL of concentrated sulphuric acid in a digestion vessel, which was placed in a pre-heated oven at 250 °C for 4 h. Scheme 1 summarizes the different steps involved in the chosen strategy. Thereafter, the obtained acid slurry was mixed with 180 mL of deionised water in a 500 mL beaker. The mixture was heated at 85 °C under stirring for 30 min, hot filtered and the FA residue was washed three times with 100 mL boiling deionised water. The filtrate was retained to recover Al. The black magnetic extract (magnetic extract) that accumulated onto the magnetic bar during stirring was collected and dried overnight at 60 °C. The solid FA residue, named PL, was dried overnight in an oven at 80 °C and used in the synthesis of ZSM-5 zeolite.

2.3. Extraction of aluminium

All the filtrates obtained during the washing of PL were transferred to a beaker and heated for 15 min at 115 °C. Thereafter, the mixture was allowed to cool down overnight at room temperature, during which a precipitate (precipitate 1) was formed, which was filtered out of the solution, air dried overnight at 70 °C and then calcined at 850 °C for 2 h. The remaining filtrate was allowed to stand for 48 h. During this time, a second white precipitate

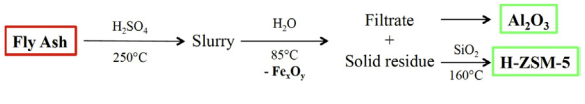

Scheme 1. From fly-ash to valuable alumina or zeolite materials.

(precipitate 2) was formed, which was filtered, dried overnight at 70 °C and then calcined at 850 °C for 2 h in order to ensure the total transformation of $Al_2(SO_4)_3$ to Al_2O_3.

2.4. Synthesis of ZSM-5_{PL2} zeolite from the solid residue of acid treated fly ash (PL)

PL (0.75 g) was mixed with 1 g of TPABr, 0.75 g of fumed silica, and 0.25 g of NaOH in 20 mL of deionised water. The obtained gel mole ratio was as follows: Si: 5.8; Al: 1.0; Na: 1.7; TPABr: 0.9; H_2O: 306.9. The latter gel was first aged at room temperature for 2 h and then submitted to a hydrothermal synthesis at 160 °C for 72 h. The obtained solid product (Na-ZSM-5_{PL2}) was filtered, washed with deionised water, dried in an oven at 70 °C and calcined at 550 °C (heating ramp 15 °C/min) for 3 h. Thereafter, Na-ZSM-5_{PL2} was ion-exchanged in 0.5 M NH_4NO_3 solution (zeolite: NH_4NO_3 ratio 1:10) at 80 °C for 1 h. The treatment with NH_4NO_3 was repeated four times with a fresh NH_4NO_3 solution each time, the solid sample obtained was dried overnight at 100 °C and calcined at 550 °C for 3 h. The so-obtained H-ZSM-5_{PL2} was characterised and used as the catalyst in the Methanol-to-Olefin (MTO) reaction.

2.5. Oxalic acid post-treatment of the as synthesized H-ZSM-5_{PL2}

One gram of the as-obtained orange-brownish zeolite (H-ZSM-5_{PL2}) from the process described in Section 2.4 was suspended in 20 mL of a 1 M oxalic acid aqueous solution. This suspension was refluxed (95 °C) for 1 h. The mixture was then cooled and filtered over a nylon membrane. An orange-brownish liquid fraction and a white powder were obtained. The latter H-ZSM-$5_{PL2\text{-}OA}$ was then calcined at 550 °C for 4 h to burn out any retained oxalic acid molecules.

2.6. BrØnsted acid site titration of H-ZSM-5_{PL2} using the H/D exchange isotope technique

The acidity of H-ZSM-5_{PL2} was determined according to the method developed by Louis et al. [22]. H-ZSM-5_{PL2} (200 mg) was activated under N_2 flow (60 mL/min) at a heating rate of 15 °C/min and held at 450 °C for 1 h to desorb water. The temperature was lowered to 200 °C, to allow D_2O vapour to pass through the solid for 1 h under N_2 flow. Dry N_2 flow was then applied to sweep away the excess of D_2O for 1 h. The titration of O-D sites was performed by back-exchanging deuterium (D) present on the surface of H-ZSM-5_{PL2} with H_2O vapour saturated N_2 stream for 1 h. Partially deuterated H_xOD_y was collected in a cold trap at −78 °C, weighed and mixed with 0.6 mL of trifluoroacetic anhydride. A $CHCl_3/CDCl_3$ reference (10:1 in weight) was prepared to determine the BrØnsted acid site density using a Bruker UltraShield 300 MHz/54 mm spectrometer.

2.7. Methanol to olefins (MTO) catalytic reaction

The zeolite catalyst (H-ZSM-5_{PL2}, H-ZSM-$5_{PL2\text{-}OA}$ or H-ZSM-5_{5524}), 60 mg, was placed in a fixed bed quartz reactor and heated at 400 or 450 °C (heating ramp 15 °C/min). After desorption of physisorbed water for 1 h, the reactor was connected to a stripper, kept at 0 °C, containing methanol. Methanol was fed to the reactor by N_2 flow (20 mL/min), resulting in a WHSV of 1.12 h^{-1}. Gas product samples (1 mL) were collected regularly during 24 h and analysed using a Hewlett Packard 5890 Gas Chromatograph (GC) equipped with a PONA column and a FID. The percentages of methanol conversion and the selectivities toward the different alkenes, alkanes and aromatics were determined as already reported elsewhere [20,21].

2.8. Characterisation techniques

The X-ray fluorescence (XRF) analysis, used to determine the elemental composition of the samples, was carried out on a Philips 1480 X-ray spectrometer. A PANanalytical X-ray diffractometer with a PW3830 generator was used for X-ray diffraction (XRD). The ZSM-5 phase purity (or % XRD crystallinity) was estimated by using the formulation suggested by Nicolaides [32], based on the seven most intense reflections:

$$\%\text{XRD crystallinity} = \frac{\sum \text{peak intensities of ZSM5 in the sample}}{\sum \text{peak intensities of the reference}} \times 100$$

The morphology of the samples was investigated using a Hitachi X-650 Scanning Electron Micro-analyser (SEM) with a CDU-lead detector. The specific surface areas of the samples were determined using Autosorb IQ Automated Gas Sorption Analyser. ^{27}Al solid state MAS NMR was performed to distinguish between the framework and extra-framework aluminium using Bruker Ascend TM 500.

3. Results and discussion

3.1. Elemental composition and morphological analysis of fly ash and acid treated FA

The elemental composition of pristine coal fly ash (FA) and after acid treatment (PL) was determined by XRF (Fig. 1). Likewise, the SEM micrographs of FA and PL are shown in Fig. 1. Sulphuric acid extracted metal oxides from FA; which caused the mass percentage of Al_2O_3, Fe_2O_3, CaO and MgO in the fly ash to decrease from 28.00 ± 0.15 % to 24.59 ± 0.06%, from 5.03 ± 0.06 % to 1.61 ± 0.01%, from 4.01 ± 0.06 % to 2.87 ± 0.10%, and 1.20 ± 0.01 % to 0.44 ± 0.00%, respectively. From these results, it can be deduced that 12% and 68% of Al_2O_3 and Fe_2O_3 were extracted from their total available content in FA, whilst Lai-Shi et al. reported that 87% of Al_2O_3 extraction from FA could be achieved after concentrated sulphuric acid (ratio acid/FA 5:1) harsh treatment at 210 °C for 80 min [23]. However, several studies are in disagreement with this former report. For example, Vassilev et al. [24] showed that sintering, hydrothermal, acidic and alkaline treatments and some physical separation technologies for bulk FA processing were commonly ineffective, expensive or harmful to the environment. Furthermore, Liu et al. [7] and Yao et al.

	Mass percentage (%)	
	FA	PL
SiO_2	59.0±0.3	68.4±0.1
Al_2O_3	28.0±0.2	24.6±0.1
Fe_2O_3	5.0±0.1	1.6±0.0
CaO	4.0±0.1	2.9±0.1
TiO_2	1.7±0.0	1.4±0.0
MgO	1.2±0.0	0.5±0.0
K_2O	0.7±0.0	0.5±0.0
P_2O_5	0.4±0.0	0.1±0.0

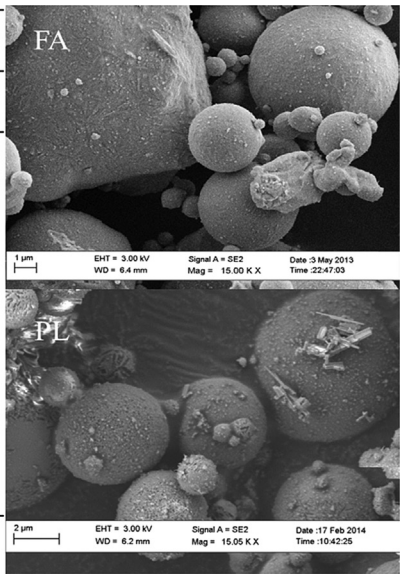

Fig. 1. Elemental composition ($n = 3$) and SEM micrographs of pristine fly ash (FA) and sulphuric acid treated FA (PL).

[9] reported that the sintering of FA with CaO at temperatures ranging between 1000 and 1200 °C, prior to acid treatment, was necessary to recover 70–90 % of Al_2O_3. These results seem to be corroborated by a study done by Shemi et al. showing that a temperature of 1150 °C was required during the sintering stage in order to extract 85% of Al from FA [25]. The important decrease in Fe_2O_3 mass percentage from 5.03 ± 0.06 % to 1.61 ± 0.01% corroborated what was reported in the literature about the recovery of iron from FA that was relatively simple and could be performed by magnetic separation [26].

The SEM images showed that there was no remarkable difference between FA and PL particles. The acid treatment could not alter the large, spherical glassy particles of coal FA which seemingly contained most of the aluminium. This might explain why only 12% of the total available Al_2O_3 content was extracted from FA under applied conditions.

3.2. Characterisation of extracted metals

Fig. 2 shows the SEM micrographs and elemental compositions of FA extracted fractions containing metals: precipitate 1, precipitate 2 and magnetic extract. It could be observed that precipitate 1 and magnetic extract were made of particles with different shapes and sizes, whilst precipitate 2 was mainly composed of homogeneous micron-sized cubic crystals.

Precipitate 1 and magnetic extract are composed of more than one metal oxide, which might derive from different mineral phases and explain the lack of homogeneity in the particles. In contrast, precipitate 2 contains aluminium as the sole metal. Shcherban et al. extracted aluminium and iron from coal FA and reported that the aluminium extract contained 86% of Al_2O_3, while the magnetic extract contained 58–66 % of Fe_3O_4 and Fe_2O_3 whereas the non-magnetic residues contained 2.6–3.6 % of Fe_2O_3 [26]. Therefore, the magnetic extract of the present study has been enriched with iron oxides by applying further separation steps during the magnetic extract and precipitate 1. One may suggest a potential use of Fe and Al extracts in the synthesis of doped Fe-zeolites and high aluminium content zeolites, respectively [27,28].

Fig. 3 shows the XRD patterns of precipitate 1, precipitate 2 and magnetic extract. It could be seen that the precipitate 1 pattern exhibits mainly $CaSO_4$, Fe_2O_3 and mullite crystalline phases. The precipitate 2 pattern exhibits the sole presence of the quasi-amorphous Al_2O_3 phase.

In the magnetic extract, characteristic reflections of Fe_2O_3, Fe_3O_4 and a small fraction of the residual mullite phase were detected. These results are in line with the SEM analysis as well as elemental composition analyses (Fig. 2).

3.3. Characterisation of H-ZSM-5_{PL2} zeolite

The elemental composition obtained by XRF analysis and SEM image of H-ZSM-5_{PL2} are given in Fig. 4. Si and Al were the main elements found and Si/Al = 6. Besides, H-ZSM-5_{PL2} also contains other elements such as Na, Ca, Fe, K and Mg. The SEM image shows that the H-ZSM-5_{PL2} morphology was mixed size range of spherulitic particles of ZSM-5 zeolite and the amorphous phase. Petrik et al. reported that tetrapropylammonium bromide could direct the formation of ZSM-5 particles with a spherulitic shape [15]. This is in agreement with the shape of ZSM-5 particles found in the present study. Na-ZSM-5_{PL2} zeolite was transformed to H-ZSM-5_{PL2} by carrying out ion exchange four times in 0.5 M of NH_4NO_3 solution followed by calcination at 550 °C for 3 h. The concentration of exchangeable cations (Na^+, Ca^{2+}, K^+ and Mg^{2+}) in the supernatants obtained after each sequential treatment with a fresh NH_4NO_3 solution was determined by ICP analysis (Fig. 5). It is noteworthy that sodium was the most abundant cation, followed by calcium and potassium. The ion-exchange efficiency was extremely high for the latter cations, while

Magnetic extract	Element	Atomic %
	O	64.0±3.0
	Fe	17.7±1.1
	Si	11.6±1.2
	Al	5.9±0.9
	Ca	0.7±0.1
Precipitate 2	**Element**	**Atomic %**
	O	62.7±0.8
	Al	35.8±0.4
	S	0.9±0.2
	Mg	0.6±0.5
Precipitate 1	**Element**	**Atomic %**
	O	55.8±2.5
	Fe	18.4±6.2
	Al	16.0±2.4
	Ca	3.0±2.9
	S	2.5±1.6
	Si	1.9±0.7
	Mg	1.4±1.3
	Ti	1.1±0.4

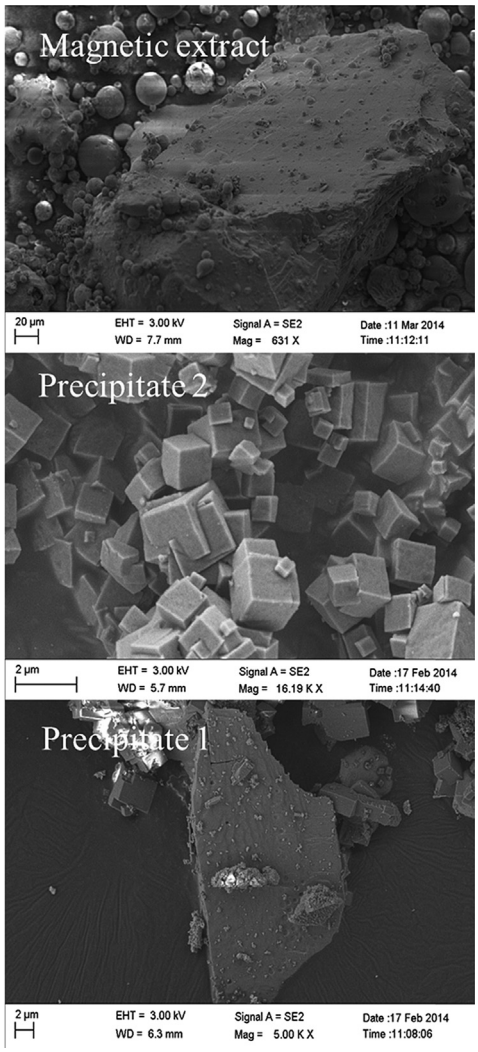

Fig. 2. Elemental composition by EDS ($n = 6$) and SEM images of precipitate 1, precipitate 2 and magnetic extract.

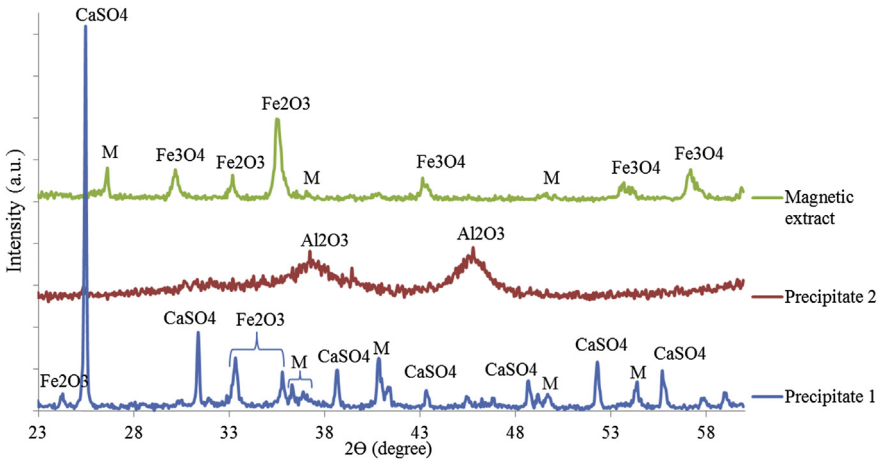

Fig. 3. XRD patterns of precipitate 1, precipitate 2 and magnetic extract (M = mullite).

Element	Atomic (%)
Si	39.7±1.1
Al	6.8±0.5
Na	1.1±0.2
Fe	0.6±0.1
Ca	0.3±0.0
K	0.1±0.0

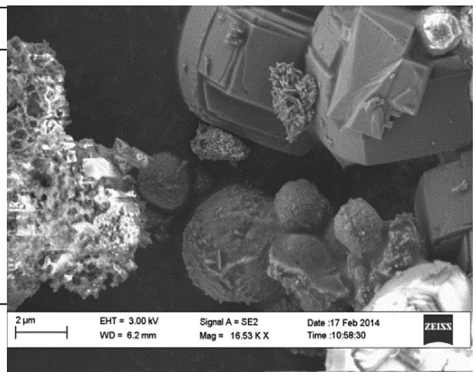

Fig. 4. Elemental composition by XRF ($n = 3$) and SEM image of H-ZSM-5_{PL2}.

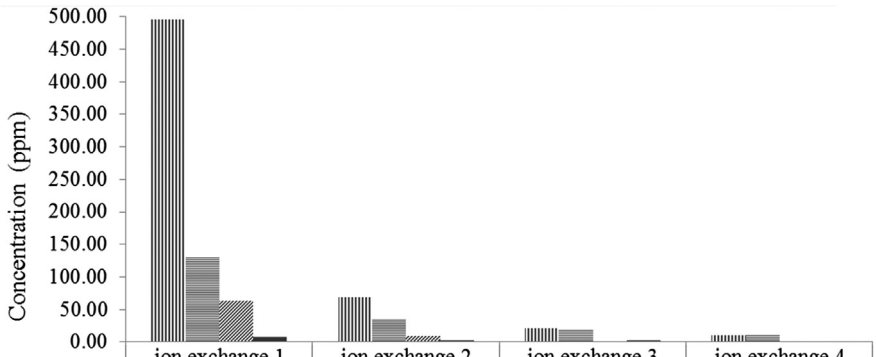

	ion exchange 1	ion exchange 2	ion exchange 3	ion exchange 4
Na	495.48	68.34	21.57	10.24
Ca	131.93	35.87	18.58	11.39
K	63.32	9.02	2.45	1.06
Mg	7.91	3.06	1.92	1.17

Fig. 5. Concentration of cations exchanged from Na-ZSM-5_{PL2} in 0.5 M NH_4NO_3 solution.

magnesium could not be easily exchanged. Kirov and Filizova investigated the influence of extra-framework cations (Na^+, K^+, Ca^{2+} and Mg^{2+}) and water in the zeolitization process. They concluded that Ca^{2+}, Na^+ and Mg^{2+} governed the stability of large channels in ZSM-5 thanks to their high hydration capacity and their location in the channels [29]. In parallel, Petrik reported that K^+ is a structure-breaking cation and hinders the zeolitization process [30]. However, the complexity of the bulk composition of coal FA renders it difficult to relate anything significantly to a particular component [24], except to note that the as-made ZSM-5 zeolite is not in Na-form only but has divalent cations present as well.

The XRD patterns of pristine fly ash (FA), acid treated FA (PL), fly ash-based ZSM-5 zeolite (H-ZSM-5_{PL2}) and commercial ZSM-5 zeolite (H-ZSM-5_{5524}) were compared in Fig. 6. FA is mainly composed of mullite, quartz and hematite phases (Fig. 6). The amorphous glassy phase in FA was identified as a hump in the background observed between 2θ 18 and 33°. Mullite, quartz and haematite phases are still present after the treatment with sulphuric acid as shown in the PL pattern. Some calcium sulphate phases could also be detected at $2\theta = 25.4°$. Characteristic reflections of the ZSM-5 zeolite phase are present in H-ZSM-5_{PL2} at 2θ: 7.7, 8.9, 13.8, 14.6, 15.8, 23, 23.9, 24.4, 29, 29.7, 44.9 and 45.4°, as shown in the simulated XRD powder patterns [31].

The zeolite phase purity in H-ZSM-5_{PL2} was found to be 62% with respect to H-ZSM-5_{5524}, set as a reference based on ZSM-5 peaks at 7.7, 8.9, 23, 23.9, 24.4, 29.7, 44.9 and 45.4°. As shown in the XRD patterns, a small amount of mullite, quartz and haematite phases were still present in the H-ZSM-5_{PL2} composite material. Querol et al. reported that the conversion efficiencies of FA into zeolites depend on the content of non-reactive phases such as haematite and resistant aluminium-silicate phases such as mullite and quartz. The dissolution rate of Al- and Si-bearing phases is as follows: glass > quartz > mullite [33,34]. Chareonpanich et al. produced a 43% containing ZSM-5 from lignite FA plus roughly 20% of unreacted Al_2O_3 [5].

The location of aluminium in H-ZSM-5_{PL2} was investigated by comparing the ^{27}Al MAS NMR spectrum to commercial H-ZSM-5_{5524} (Fig. 7). Two signals were observed in H-ZSM-5_{PL2} and H-ZSM-5_{5524} zeolite spectra: a weak signal at 0 ppm corresponding to non-framework Al (octahedral coordination) and an intense signal at 55 ppm

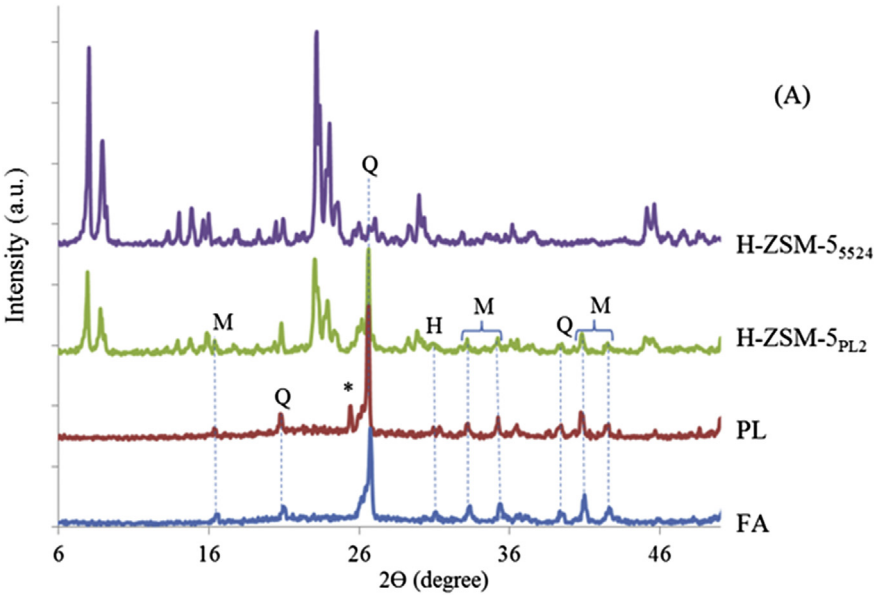

Fig. 6. XRD patterns of FA, PL, H-ZSM-5$_{PL2}$ and commercial H-ZSM-5$_{5524}$ (M = mullite, Q = quartz, H = haematite and (*) = calcium sulphate).

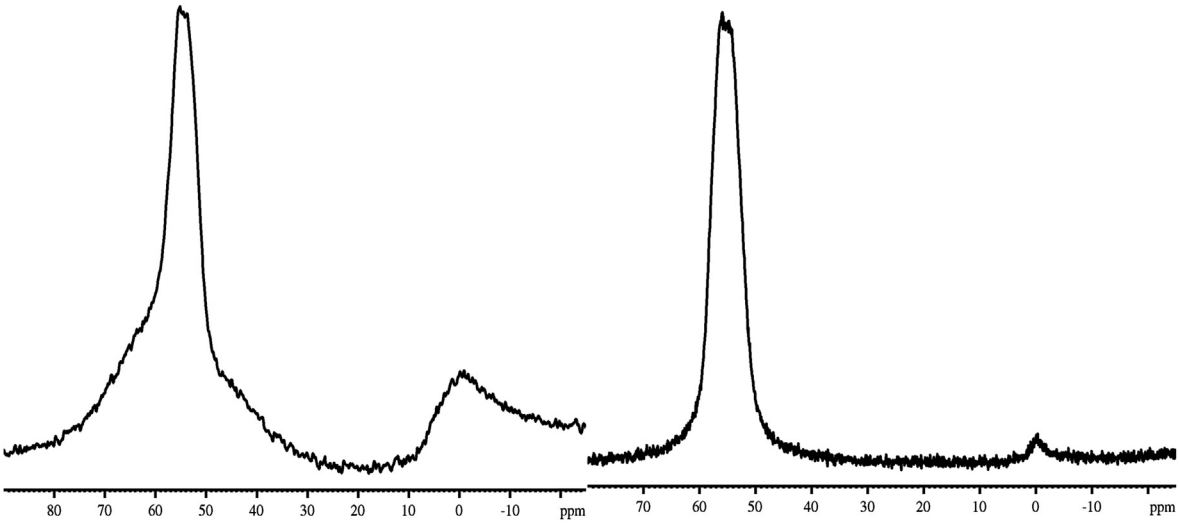

Fig. 7. ^{27}Al MAS NMR spectra of H-ZSM-5$_{PL2}$ (left) and H-ZSM-5$_{5524}$ (right).

corresponding to tetrahedral framework Al. The tetrahedral Al signal of H-ZSM-5$_{5524}$ was narrower than of H-ZSM-5$_{PL2}$. Similar results about the location of Al in MFI zeolite were reported by Triantafyllidis et al. and Sazama et al. [35,36].

Louis et al. developed a relation between the acid site density (mmol $H^+/g_{zeolite}$) and the theoretical Si/Al mole ratio in ZSM-5 [23], which allowed an estimation of H-ZSM-5$_{PL2}$ and H-ZSM-5$_{PL2\text{-}OA}$ acidities. Indeed, the zeolite phase present in the H-ZSM-5$_{PL2}$ sample has a predicted Si/Al = 22. This is one of the main reasons why it was selected to compare the catalytic behaviour of FA-converted materials with the commercially available, reportedly active MTO catalyst exhibiting roughly the same Si/Al = 25 [21b–e].

As mentioned earlier, the Methanol-to-Olefin (MTO) reaction was mainly used as the probe reaction to validate the synthesis of ZSM-5 zeolite catalyst starting from acid treated FA. Table 1 presents the chemical and physical properties (Si/Al ratio, number of acid sites, BET surface area) of PL, H-ZSM-5$_{PL2}$ and H-ZSM-5$_{5524}$ zeolites. It could be seen that the Si/Al molar ratio and BET surface area of PL were 2 and 3 m^2/g, respectively. This starting material exhibited a low activity in MTH; and was able to convert methanol only into aromatics as no olefins could be detected (Table 2). This unusual aromatization behaviour might be related to the presence of traces of different metals in PL. The Si/Al ratio of H-ZSM-5$_{PL2}$ is roughly 6 which remain far below the lowest Si/Al of 11 found in

Table 1
Si/Al ratio, number of acid sites and BET surface area for PL, H-ZSM-5_{PL2}, H-ZSM-$5_{PL2\text{-}OA}$ and H-ZSM-5_{5524}.

	PL	ZSM-5_{PL2}	ZSM-$5_{PL2\text{-}OA}$	ZSM-5_{5524}
Si/Al ratio	2	5.8	6.3	25(*)
Number of acid sites (mmol $H^+/g_{zeolite}$)	/	0.61	0.31	0.86
BET surface area (m^2/g)	3	328	–	480

(*) = data supplied by Zeolyst.

ZSM-5 zeolites [14]. Beside the Si/Al molar ratio, the presence of mullite and other unreacted FA phases affected the number of acid sites, BET surface area and methanol conversion (Tables 1 and 2). H-ZSM-5_{PL2} is less active than H-ZSM-5_{5524} (which exhibits full methanol conversion) and also deactivates after 5 h on stream with a methanol conversion drop from 60% (after 1 h) to 52% (after 2.5 h) (Fig. 8). The increase in reaction temperature in the case of H-ZSM-5_{PL2} from 400 to 450 °C initially led to a higher conversion and rapid catalyst deactivation (Fig. 8). The deactivation of H-ZSM-5_{PL2} is probably due to the low Si/Al molar ratio and BET surface area [37,38]. An easy and cheap post-synthetic treatment using oxalic acid was used in order to optimize the MTO performance of the fly ash-based ZSM-5 zeolite. Oxalic acid has been chosen since it is a potent chelating agent, broadly used in zeolite post-synthesis treatments to extract extra-framework aluminium species (EFAl) or to generate a certain mesoporosity [39]. Herein, it is reasonable to assume that oxalic acid will mainly chelate and extract residual non crystallised metal cations, since the latter are probably responsible for catalyst instability; removing them would improve the catalyst performance of FA-derived zeolites.

Fig. 9 shows the preliminary MTO results comparing acid-treated H-ZSM-$5_{PL2\text{-}OA}$ with H-ZSM-5_{PL2} and H-ZSM-5_{5524} catalysts. The catalyst activity was significantly improved and full methanol conversion could now be achieved and kept during 20 h on stream ($X_{methanol} > 95\%$). This enhancement of FA-prepared zeolite catalyst viability is accompanied by extremely promising selectivities toward light olefins (Table 2). Indeed, 35% of propylene and 66% of C_2–C_4 olefins were produced over H-ZSM-$5_{PL2\text{-}OA}$, whilst only 19% and 44% were obtained over H-ZSM-5_{5524} catalyst.

The strategy to design FA-prepared ZSM-5 zeolites for acid-catalysed purposes appears valid and promising. The conversion of methanol into hydrocarbons is depicted in Table 3. In spite of improving the cumulative methanol conversion capacities from 30 g to 71 g depending on H-

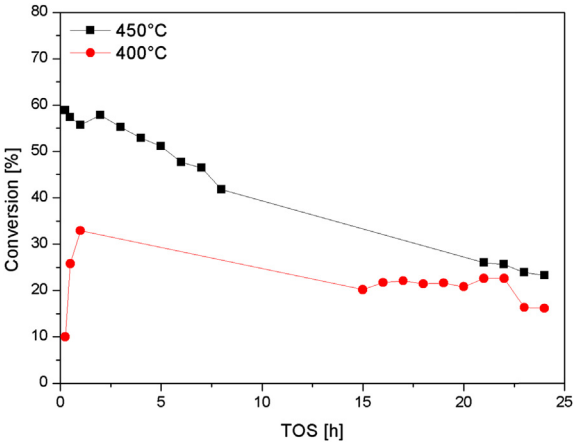

Fig. 8. H-ZSM-5_{PL2} behaviour in the MTO reaction at 400 and 450 °C.

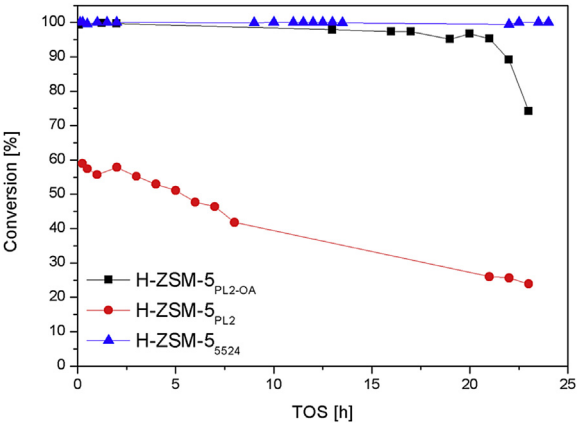

Fig. 9. Comparison between ZSM-5 zeolites in the MTO as a function of time on stream at 450 °C.

Table 3
Cumulative methanol conversion capacities and light olefins productivities for the three zeolites.

Entry	Zeolite	χ [g($MeOH_{converted}$)/g(catalyst)]	π[g($C_{2=}$–$C_{4=}$)/g(catalyst)]
1	H-ZSM-5_{PL2}	30	5
2	H-ZSM-$5_{PL2\text{-}OA}$	71	21
3	H-ZSM-5_{5524}	212 [20b]	41 [20b]

Table 2
MTO conversion and selectivity data for the different catalysts.

Zeolite	Conversion [%]	Selectivities [%]					
		CH_4–C_4H_{10}	$C_{2=}$	$C_{3=}$	$C_{4=}$	$C_{5=}$	C_{6+} – aromatics
PL	≈5	0	0	0	0	0	100
H-ZSM-5_{PL2}	58	50	17	20	4	4	5
H-ZSM-$5_{PL2\text{-}OA}$	100	5	17	35	14	15	14
H-ZSM-5_{5524}	100	20	12	19	13	14	22

Results obtained under the following reaction conditions: temperature 450 °C, after 1 h on stream, with a WHSV of 1.12 h^{-1}.

ZSM-5_{PL2} or H-ZSM-$5_{PL2\text{-}OA}$ catalyst, it is still not competing with the 212 g converted over H-ZSM-5_{5524} catalyst. Further work is therefore required to improve the FA-prepared ZSM-5 catalyst life time by optimisation of the post-treatments.

4. Conclusion

This study highlights a strategy to valorise South African coal fly ash (after metals extraction which might be recovered and valorised as well) as a feedstock for the synthesis of ZSM-5 zeolite. From raw fly-ash, a FA-zeolite composite was successfully prepared, containing 62% of pure ZSM-5 phase and 0.61 mmol BrØnsted acid sites per $g_{zeolite}$. Interestingly, this FA-ZSM-5 composite successfully behaves as a catalyst in the MTO reaction. In order to enhance its activity and stability, a cheap oxalic acid post-treatment has been undertaken to achieve full-methanol conversion during 15–20 h on stream. In addition, H-ZSM-$5_{PL2\text{-}OA}$ led to reach a 35% propylene selectivity and 66% light olefins (C_2–C_4) selectivity.

Acknowledgements

The financial support of the NRF Protea program, the technical and material supports of the Environmental and Nano Sciences (ENS) are gratefully acknowledged. PL would like to thank the National Research Fund Luxembourg for his PhD Grant (5898454).

References

[1] M.A. Ahmaruzzaman, Process Energy Combust. Sci. 36 (3) (2010) 327–363.
[2] L.F. Petrik, R.A. White, M.J. Klink, V.S. Somerset, C.L. Burgers, M.V. Fey, Utilization of South African Fly Ash to Treat Acid Coal Mine Drainage and Production of High Quality Zeolites from the Residual Solids, International Ash Utilization Symposium, Lexington, KY, 2003.
[3] G. Madzivire, W.M. Gitari, V.R.K. Vadapalli, T.V. Ojumu, L.F. Petrik, Miner. Eng. 24 (14) (2011) 1467–1477.
[4] N.M. Musyoka, L.F. Petrik, W.M. Gitari, G. Balfour, E. Hums, J. Environ. Sci. Health, Part A 47 (2012) 337–350.
[5] M. Chareonpanich, T. Namto, P. Kongkachuichay, J. Limtrakul, Fuel Process. Technol. 85 (2004) 1623–1634.
[6] A. Hernandez-Exposito, J.M. Chimenos, A.I. Fernandez, O. Font, X. Querol, P. Coca, G.F. Pena, Chem. Eng. J. 118 (2006) 69–75.
[7] K. Liu, J. Xue, J. Zhu, Light Met. (2012) 201–206.
[8] J.W. Hosterman, S.H. Patterson, E.E. Good, World Non Bauxite Aluminium Resources Excluding Alunite, U.S. Government Printing Office, Washington, DC, 1990, p. 51.
[9] Z.T. Yao, M.S. Xia, P.K. Sarker, T. Chen, Fuel 120 (2014) 74–85.
[10] M. Paul, M. Seferinoglub, G.A. Ayçikc, A. Sandströmd, J. Paul, Div. Fuel Chem. 49 (2004) 978–982.
[11] A.S. Shoumkova, Waste Manag. Res. 29 (10) (2011) 1078–1089.
[12] (a) N.M. Musyoka, L.F. Petrik, O.O. Fatoba, E. Hums, Miner. Eng. 53 (2013) 9–15;
(b) A. Grela, M. Hebda, M. Lach, J. Miku, Micropor. Mesopor. Mater. 220 (2016) 155–162.
[13] Y. Kuwahara, T. Ohmichi, T. Kameqawa, K. Mori, H. Yamashita, J. Mater. Chem. 20 (2010) 5052–5062.
[14] F.J. van Der Gaag, J.C. Jansen, H. van Bekkum, Template Variation in the Synthesis of Zeolite ZSM-5, Laboratory of Organic Chemistry; Delft University of Technology, Delft, The Netherlands, 1985.
[15] L.F. Petrik, C.T. O'Connor, S. Schwarz, The Influence of Various Parameters on the Morphology and Crystal Size of ZSM-5 and the Relationship Between Morphology and Crystal and Propene Oligomerization Activity, in: H.K. Beyer, H.G. Karge, I. Kiricsi, J.B. Nagy (Eds.), Catalysis by Microporous Materials: Studies in Surface Science and Catalysis, Proceedings of ZEOCAT '95, Szombathely, Hungary, vol. 94, 1995, pp. 517–524.
[16] H.T. Tuan, I.K. Bae, Y.N. Jang, S.C. Chae, Y.B. Chae, D.S. Suhr, J. Ceram. Process. Res. 11 (2) (2010) 204–208.
[17] C. Martinez, J. Perez-Pariente, Zeolites and Ordered Porous Solids: Fundamentals and Applications, 3rd Feza School on Zeolites & 5th International Feza Conference, Valencia, Spain, 2011.
[18] S. Narayanan, A. Sultana, K. Krishna, P. Meriaudeau, C. Naccache, Catal. Lett. 34 (1–2) (1995) 129–138.
[19] A.N. Kalyankar, A.L. Choudhari, A.A. Joshi, Int. J. Basic Appl. Res. 1 (2011) 59–63.
[20] (a) F.L. Bleken, S. Chavan, U. Olsbye, M. Boltz, F. Ocampo, B. Louis, Appl. Catal. A Gen. 447–448 (2012) 178–185;
(b) P. Losch, M. Boltz, C. Bernardon, B. Louis, A. Palcic, V. Valtchev, Appl. Catal. A 509 (2015) 30–37;
(c) P. Losch, G. Laugel, J.S. Martinez-Espin, S. Chavan, U. Olsbye, B. Louis, Top. Catal. 58 (2015) 826–832.
[21] (a) U. Olsbye, S. Svelle, M. Bjørgen, P. Beato, T.V.W. Janssens, F. Joensen, S. Bordiga, K.P. Lillerud, Angew. Chem. 51 (24) (2012) 5810–5831;
(b) M. Stöcker, Microporous Mesoporous Mater. 29 (1999) 3–48;
(c) C.D. Chang, C.T.W. Chu, R.F. Socha, J. Catal. 86 (2) (1984) 289–296;
(d) M. Boltz, P. Losch, B. Louis, Adv. Chem. Lett. 1 (2013) 247–256;
(e) P. Losch, M. Boltz, B. Louis, S. Chavan, U. Olsbye, C. R. Chimie 18 (2015) 330–335;
(f) D. Xiang, Y. Qian, Y. Man, S. Yang, Appl. Energy 113 (2014) 639–647.
[22] B. Louis, S. Walspurger, J. Sommer, Catal. Lett. 93 (1–2) (2004) 81–84.
[23] L. Lai-Shi, W. Yu-Sheng, L. Ying-Ying, Z. Yu-Chun, Chin. J. Process Eng. 11 (2) (2011) 254–258.
[24] S.V. Vassilev, R. Menendes, D. Alvarez, M. Diaz-Somoano, M.R. Martinez-Tarazona, Fuel 82 (2003) 1793–1811.
[25] A. Shemi, Extraction of Aluminium from Coal Fly Ash using a Two-step Acid Leach Process, Master thesis, University of Witwatersrand, Johannesburg, South Africa, 2013.
[26] S. Shcherban, V. Raizman, I. Pevzner, Div. Fuel Chem. 40 (4) (1995) 863–867.
[27] G. Lv, Z. Li, W.T. Jiang, C. Ackley, N. Fenske, N. Demarco, Chem. Eng. Res. Des. 92 (2) (2014) 384–390.
[28] N.M. Musyoka, L.F. Petrik, E. Hums, H. Baser, W. Schwieger, Catal. Today 190 (1) (2012) 38–46.
[29] G. Kirov, L. Filizova, Bulg. Mineral. Soc. 49 (2012) 65–82.
[30] L. Petrik, South Afr. J. Sci. 105 (2009) 251–257.
[31] M.M.J. Treacy, J.B. Higgins, Collection of Simulated XRD Power Patterns for Zeolites, 4th ed., Elsevier, 2001.
[32] C.P. Nicolaides, Appl. Catal. A 185 (1999) 211–217.
[33] X. Querol, N. Moreno, J.C. Umaña, A. Alastuey, E. Hernández, A. López-Soler, F. Plana, Int. J. Coal Geol. 50 (2002) 413–423.
[34] D. Voll, P. Angerer, A. Beran, H. Schneider, Vib. Spectrosc. 30 (2002) 237–243.
[35] K.S. Triantafyllidis, L. Nalbandian, P.N. Trikalitis, A.K. Ladavos, T. Mavromoustakos, C.P. Nicolaides, Micropor. Mesopor. Mater. 75 (2004) 89–100.
[36] P. Sazama, B. Wichterlova, J. Dedecek, Z. Tvaruskova, Z. Musilova, L. Palumbo, S. Sklenak, O. Gonsiorova, Micropor. Mesopor. Mater. 143 (2011) 87–96.
[37] D. Chen, K. Moljord, A. Holmen, Micropor. Mesopor. Mater. 164 (2012) 239–250.
[38] D. Mores, J. Kornatowski, U. Olsbye, B.M. Weckhuysen, Chem. A Eur. J. 17 (10) (2011) 2874–2884.
[39] M. Müller, G. Harvey, R. Prins, Micropor. Mesopor. Mater 34 (2000) 135–147.